Development of a Chemical-free Floatation Technology for the Purification of Vein Graphite and Characterization of the Products

Gamaralalage R. A. Kumara (grakumara2000@yahoo.com)
National Institute of Fundamental Studies
Herath Mudiyanselage G. T. A. Pitawala
University of Peradeniya
Buddika Karunarathne
National Institute of Fundamental Studies
Mantilaka Mudiyanselage M. G. P. G. Mantilaka
University of Peradeniya
Rajapakse Mudiyanselage G. Rajapakse
University of Peradeniya
Hsin-Hui Huang
Toyota Technological Institute
K. Kanishka H. De Silva
Toyota Technological Institute
Masamichi Yoshimura
Toyota Technological Institute

Research Article

Keywords: chemical-free floatation technology, purification, vein graphite, products, Graphite

Posted Date: September 30th, 2021

DOI: https://doi.org/10.21203/rs.3.rs-942235/v1

Version of Record: A version of this preprint was published at Scientific Reports on November 22nd, 2021.
See the published version at https://doi.org/10.1038/s41598-021-02101-9.

Abstract

A novel and simple flotation technique has been developed to prepare high-purity graphite from impure graphite. In this method, a suspension of powdered graphite (PG) is dispersed and stirred in water without adding froth formers or supportive chemicals. This makes fine particles of graphite to move upwards and float on water. X-ray diffraction (XRD) analysis reveals that the floated graphite (FG) has a lower c-axis parameter, indicating the removal of interlayer impurities. A notable increase in the intensity ratio of the D band to G band in the Raman spectra indicates that the FG has more edge defects due to their smaller crystallite sizes. Transmission electron microscopic (TEM) analysis shows the number of layers in FG has been reduced to 16 from 68 in PG. The absence of C = O vibration of Fourier Transformed Infrared (FT-IR) spectroscopy in treated and untreated samples suggests that layers of them are not significantly oxidized. However, X-ray photoelectron spectroscopic (XPS) analysis shows the presence of C-O-C ether functionalities, possibly on edge planes. Further, the product has higher purity with increased carbon content. Therefore, the technique is useful in the value enhancement of graphite, the reduction of the chemical cost of the conventional techniques, environmental friendliness, and improvement of its applications.

Introduction

Graphite is one of the astounding naturally occurring materials that is characterized by its inherent specific properties such as low hardness, metallic lustre, high lubricity, refractoriness, high heat and electrical conductivities, thermal resistance and inertness. These properties of graphite make it an extremely attractive material for many technological applications. Hence, graphite has a remarkably high industrial applicability which none of the other naturally occurring substance would have up to the extent that graphite has. Naturally occurring graphite has a wide range of purities depending on their geological occurrence.[1]

Demand for high purity graphite is progressively increasing in the recent past due not only to its versatile traditional applications but also to innumerable novel applications that researchers foresee, in the near future, for graphite and graphene products. Basically, naturally occurring graphite is classified into three forms: (i) flake graphite, (ii) vein graphite and (iii) amorphous graphite.[2] Flake graphite is found in regionally metamorphosed sedimentary rocks and has a distinctly flaky morphology and is typically found as flat and plate-like masses. They are very common in many parts of the world. However, vein graphite is found only in Sri Lanka[3], India, Madagascar, USA, Canada and UK.[4]

Although, carbon content of vein graphite varieties is considered to be high up to about 90-99.8%, their natural purity is often in the lower-end of this range due to the presence of gangue minerals which are naturally associated with the graphite veins. Furthermore, the purity of natural vein graphite varies from place to place in the same deposit. Impurities are present as mineral inclusions or they are intercalated between graphite layers. Iron (Fe), Ca, Mg, Si, Al and Na are the major impurities with lesser concentrations of transition metals such as Cu, Ni, Co and Zn.[5] The presence of impurities inevitably

decrease the quality of even such highly pure vein graphite and the development of simple, low-cost, scalable and industrially-viable purification techniques are still required for better industrial utilization of natural graphite.

Several methods have been introduced to enhance the purity of graphite powders but the majority of them are based on environmentally unfriendly acid or alkali treatment processes[6] while other methods involve expansion processes and physical treatments.[7] Among these techniques, floatation is an industrially adaptable, simple, cost-effective and selective mineral processing technique.[8] The raw material concentration by floatation generally utilizes the surface physicochemical properties of water-repellent (hydrophobic) particles to enable to float with air bubbles in order to form a froth[9] and together with which fine particles move upwards and float on the water surface. Graphite is particularly suitable for this process, since, in the absence of considerable amounts of functional groups such as ether, hydroxyl and carboxyl that are formed by the ariel oxidation of valency-unsatisfied surface carbon atoms of graphite crystals, naturally occurring graphite forms with high C% are generally hydrophobic. As such, this hydrophobicity of graphite particles is used in the purification of mined graphite together with some added specific chemical reagents to help improve froth formation.[10]

Although graphite has specific gravity around 1.9–2.3, hydrophobic nature of graphite fine particles aids the floatation process when water is used as the floating medium. The contact angle in the air-water-mineral system is a measure of the hydrophobicity of a mineral surface and graphite is characterized by relatively large contact angles which depend, to some extent, on the pH of the water used and also on the characteristics of the surface preparation.[8] Graphite floatation is not new as demonstrated by Parks *et al*, Paulson *et al* and Pugh and there are ample references to this effect.[10–12] However, most of these studies are focused on the chemical composition of floated graphite, particularly, on the total carbon and trace elements. But the structural and morphological characteristics of floated graphite, which are the key properties for industrial applications, have not been evaluated. In graphite floatation, oils such as kerosene[13] and diesel[14] in combination with froth formers are used to enhance froth formation. The use of such chemicals undoubtedly complicates the purification process since all these chemicals that may have bound or adsorbed on graphite crystallites have to be removed at the final stage. Usage of chemicals has increased environmental problems due to generation of wastes, high production cost and consequent reduction of profits. As such, this process demands not only chemicals but also an intensive labour, making it industrially less attractive. Also, most of the froth formers used in the floatation of graphite are environmentally unfriendly chemicals. Therefore, if a method can be developed that does not require any chemical to float graphite on water, then that is more industrially-viable and adaptable.

In this manuscript, we reveal an effective chemical-free, simple floatation technique which we have developed in order to obtain high purity and well crystalline graphite products by floating graphite fine particles on water. Both the pristine powdered graphite (PG) and floated graphite (FG) are characterized using several independent material characterization techniques and the success of the method is explained in terms of improved physical and chemical properties of floated powdered graphite. This

method is scalable, simple and of low-cost making it industrially viable, adaptable and environmental-friendly. The developed method has enhanced the purity of graphite from 91.9 to 98% of carbon content which makes a 4–12 times value addition to raw-graphite. Therefore, the developed chemical-free floatation technique is very useful in the value enhancement of graphite, reduction of chemical cost from conventional froth floatation technique, environmental friendliness and improvement of its applications.

Results And Discussion

Figure 1 shows the XRD patterns of the PG and FG samples. A very intense and narrow peak is shown referring to X-ray reflection on the (002) plane of graphite. Intriguingly, (002) peak of the FG ($2\theta = 26.56^{o}$) shifts toward a slightly higher angle by approximately 0.04° compared to peak position of the PG ($2\theta = 26.52°$). It indicates a smaller c-axis lattice parameter of the FG (0.3353 nm) than that of the PG (0.3358 nm). Moreover, the full width at half-maximum (FWHM) of the (002) XRD peak is significantly larger in the FG. This is strongly related to the crystallite size according to the Scherrer equation, $La = 1.84\lambda/\beta.\cos\theta$, where the λ is the X-ray wavelength (0.15406 nm), θ is the position of the (002) peak, and β is the FWHM of the (002) peak in 2θ (rad) units. Thus, the crystallite size of the FG and PG were calculated to be approximately 86 nm and 101 nm, respectively. However, the intrinsic instrumental broadening should also be considered when elucidating exact values. A slight decrease in interlayer spacing suggests the removal of interlayer species that are present in low quantities in pristine graphite samples. As such, XRD provides indirect evidence to assure that the floating technique can aid the enrichment of carbon percentage in graphite samples. The quantitative elemental analysis that has been performed for both samples will attest to this point (*vide infra*). The XRD analysis of flake graphite (99% Purity, Alfa Aesar) that has been performed by Abdolhosseinzadeh et al. show very similar pattern where the peak positions of flake graphite have been shifted to higher 2θ values. The (002) diffraction appears at $2\theta = 26.7^{o}$ giving a d-value of 0.3340 nm. This is further evidence to show the effect of purity on lattice parameters of graphite crystallites. Although absolute values of intensities (Is) of XRD depend on the amount of diffracting atoms present in the sample, which in turn depends on the amount of material used to get the diffractogrammes, the normalized intensities obtained by dividing I(002) by I(004) are meaningful and independent of the amount of materials used. As revealed by XRD data, the floating of ball-milled graphite has increased this intensity ratio indicating that floating of ball-milled graphite has resulted in increasing the crystallinity of the sample. It is interesting to note that ball-milling of graphite brings the crystallite sizes variable range up to nanometre scale and floating the powder in water further decreases the crystallite size by 15 nm. The decreased crystallite size and the decreased interlayer distance of the FG collectively indicate the shrinking of particles due to floating which may be due to removal of impurities in the pristine graphite when it is milled and floated in water.

We assessed the impurity contents of original graphite, PG and FG samples as well as their carbon content variation from the data given in Table 1, 2 and Fig. 2. Impurities in vein graphite can basically occur either as mineral inclusions such as quartz, pyroxene, pyrrhotite, pyrite, chalcopyrite, sphalerite, marcasite, chlorite, calcite, siderite and dolomite and copper or as elements incorporated into the

crystalline lattice[3,5,15]. Depletion of elements in low-carbon graphite indicates that most of impurities are incorporated as mineral inclusions. However, the rest of remaining such elements indicates the floated graphite still contains fine inclusion of some minerals which can be explained by EDS analysis given in Fig. 2. This shows that the mineral inclusions are present in graphite used for the present study before grinding and the carbon weight percentage around 84%. Silicate minerals such as quartz (SiO_2), pyroxene group minerals (Mg,Fe)SiO_3 or (CaxMgyFez)(Mgy1Fez1)Si_2O_6) and chalcopyrite ($CuFeS_2$) as well as native element minerals such as copper (Cu) and iron (Fe) can be suggested from EDS elemental distribution of original graphite sample (Fig. 2 and Table 1). Further, some silicate minerals with copper and iron also present in raw samples. These minerals may have formed due to the alteration process by hydrothermal fluids. However, the carbon percentage has increased in at least up to 97% as a result of removing mainly of silicate minerals during flotation process. However, the fine inclusion such as iron bearing minerals have not been fully removed and they have floated with graphite (Table 2) as some of them occur as nanometer scale minerals (see Fig. 2-b). Therefore, iron content has increased in FG samples. The enrichment of Ba in floated graphite indicates that the element is incorporated into the crystalline lattice. However, the final FG products in all products contain over 97.3% of carbon content (Table 2). Therefore final FC products are suitable for applications including nuclear reactors, furnaces, advanced materials, specific niche applications, expandable graphite products, composites and electronic applications. The final products can be marketed for USD 4000–6000 per ton according to graphite market in 2019[15]. According to elemental results in Table 2, the PG used for the study have 91-95.9% carbon content and these PG has market value of USD 500–1100 per ton. Therefore after the proposed simple floatation technique reported in this study is capable of adding 4–12 times value addition, which is a huge value addition to graphite. This can be further increased by making PG finer powders and upon development of process such as magnetic separation of iron in final FG products.

Table 1
Elemental analysis of graphite samples by EDS

Elements	C	O	Si	S	Mg	Fe	Al	Cu
Sample FG weight %	96.54	2.66	0.23	0.18	b.d	0.26	0.12	b.d
Sample FG atomic %	97.67	2.02	0.10	0.09	b.d	0.06	0.06	b.d
Sample PG weight %	84.69	9.77	4.99	b.d	0.18	0.22	n.d	0.19
Sample PG atomic %	89.81	7.78	2.26	b.d	0.06	0.05	n.d	0.04
b.d – below the detection limits, n.d – not detected								

Table 2
Compositions of the graphite samples as determined by ICP-MS analysis

Sample	Purity	Carbon Content together with some minor elemental impurities as Weight%						
		Al	K	Fe	Ca	Mg	C_{total}	
PG	High	< 0.01	< 0.01	0.03	0.05	0.01	95.9	
FG		< 0.01	< 0.01	0.09	0.01	0.01	98	
PG	Moderate	0.04	< 0.01	0.11	< 0.01	0.06	92.9	
FG		0.04	< 0.01	0.12	< 0.01	0.06	97.3	
PG	Low	0.14	< 0.01	0.21	0.09	0.14	91.9	
FG		0.09	0.01	0.14	0.03	0.09	98	
Trace Elements in ppm (Abundance is too low to be given as Weight %)								
		Ba	Bi	Cr	Cu	Mn	Mo	Pb
PG	High	7.3	1.7	6	24.6	6	0.2	1
FG		11.7	1.6	4	19.7	7	0.1	1
PG	Moderate	7.7	1.7	1	38.5	7	0.3	1.3
FG		8.1	1.6	< 1	38.1	7	< 0.1	1.5
PG	Low	6.2	0.4	14	19	31	0.6	1.3
FG		11.8	0.2	8	10.1	20	0.3	0.9

In Raman spectra, given in Fig. 3, three prominent peaks at 1347 cm^{-1}, 1579 cm^{-1}, and 2690 cm^{-1} correspond to the D band, G band, and 2D band for both PG and FG samples, respectively. Notably, the difference between two samples is the intensity ratio of the D band and G band (I_D/I_G), in which it was measured to be larger in the FG (0.10) than that of the PG (0.03) suggesting that the higher value of I_D/I_G results from the edges of graphite. In other words, with the same kind of graphite, the floated graphite has smaller crystalline size (nanographite) compared to the unfloated graphite, which is compatible with the XRD results.

The crystal structure of the PG and FG samples were further investigated by TEM analysis and the results are shown in Fig. 4 and 5, respectively. The size of the sheets ranged from 0.5 µm to 4 µm. Insets in Fig. 4(a) and 5(a) are the corresponding [001] SAED patterns. It is intriguing that distinct six-fold symmetry diffraction spots present more frequently in the FG specimen compared to the PG sample. On the other hand, the electron diffraction pattern of the PG exhibit rather ring-like reflections (polycrystalline), as shown in the inset of Fig. 5(a). It indicates that the FG shows either high crystallinity in nature or/and has

no rotational boundaries in this area. The lattice parameters of PG and FG were measured to be 0.247 and 0.246 nm, respectively. To quantify the number of layers in graphite/graphene, a commonly used method is by counting the number of folds at the edge of the flakes/sheets in high resolution TEM images (HRTEM), as shown in Fig. 4(b) and 5(b). It was measured to be more than 68 layers in PG while FG has 16 layers. The interlayer distance of PG was measure to be 0.339 nm, corresponding to (002) graphite crystal spacing. However, FG has a relatively small interlayer spacing of 0.326 nm. This is consistent with the XRD results where the (002) peak of FG shifted toward the higher 2q angle resulting in a smaller in lattice spacing.

In order to distinguish the features more easily and to remove contrast due to the presence of amorphous materials, HRTEM images were filtered by Fast Fourier Transform (FFT) method (Fig. 4(c) and 5(c)). The corresponding FFT images are shown in Fig. 4(d) and 5(d). It should be noted that the HRTEM images were taken at featureless regions, in which these might be area with few-layer graphene. The interplanar spacings along (100) planes were measured to be 0.230 nm and 0.242 nm for the PG and FG, respectively, which are closely matching with the lattice parameter calculated from the diffraction patterns. However, it should be aware that the periodicity in the region might not be the original position of the spots due to the instrumental limitations.

Figure 6 depicts the FT-IR spectra of PG and FG samples. The spectra of both samples are basically very similar with a broad band between 3200 cm^{-1} to 3700 cm^{-1} resembling the O-H vibrations of adsorbed water molecules on graphite surfaces and narrow band centered at 1622 cm^{-1} due to C = C stretching of conjugated double bonds that are present in graphene layers. The absence of bands at 2925 cm^{-1} (asymmetric C-H stretching in CH_2 groups) 2855 cm^{-1} (symmetric C-H stretching in CH_2 groups) suggest that there are no detectable amounts of saturated sp^3 carbon atoms in both PG and FG samples. In other words, there are no detectable defects due to hydrogenated double bonds in both samples. Absence of C = O vibration centered at 1738 cm^{-1} shows that the unsaturated carbon atoms do not contain any carbonyl functionality and hence the materials contain only conjugated C = C in their graphene sheets.

XPS was used to monitor the changes in core level and valence band structure of the PG and FG samples. The survey scan spectra (Fig. 7) of PG (a) and FG (b) samples indicate the presence of C and O atoms. It is found that the oxygen content of the FG sample is much higher, though the absolute percentages are very small in both types, compared to the PG sample. The oxygen to carbon ratio (O/C) was measured to be 0.04 PG sample and 0.05 in FG sample. The C 1s spectra of the PG and the FG samples are shown in Fig. 7 (c) and (d). Both are fitted with four Lorentzian-Gaussian peaks of 20:80 ratios. The most intense peak, at 284.5 eV, is assigned to sp^2 C = C bonds atoms, together with the weak component at 290.1 eV that corresponds to its π- π transition (signature of graphitic carbon). The component at 286.5 eV has been usually attributed to C-O-C (ether) bonds. It is noted that two samples exhibit similar patterns. However, the C1s spectrum of floated graphite displays higher intensity of the C-O-C and C-C components and lower intensity of the C = C and π- π bonds. It is generally accepted that C-O-C bonds are formed at the edge of the graphene sheets. As shown in the Raman spectra, the higher D

peak represents to higher amounts of edges in FG sample and those edges might be the spots for C-O-C bonds to form. Table 2 shows the different bonds present in both PG and FG. With respect to PG there is 4% reduction of C = C bonds, 3% increase in C-C and 11% increase in C-O-C in FG.

The present study is the first attempt to understand the characteristics of the floated graphite in de-ionized water. This simple floatation technique has been introduced to float ground graphite particles with mineral impurities on the surface of de-ionized water and floatation has been affected with the aid of shaking. This technique does not require any froth formers or floatation aid chemicals and as such it is highly industrially viable and environmentally friendly. The powdered and floated graphite samples have some differences in their crystallite sizes, morphologies, and purities. Floatation has resulted in shrinking of crystallite size due to the removal of mineral inclusions within the interlayer spaces. Number of defects has been increased in floated graphite and both samples have some C-O-C ether bonds in slightly higher amount in the floated graphite. The number of layers present in crystallites has been remarkably decreased in floated graphite when compared to that in powdered graphite that did not subjected to floating in water. The floatation technique can remove many impurities which are present as mineral inclusions in graphite, to some extent. The floatation aids the remarkable enhancement of carbon content in graphite samples and is more prominent when the original samples are impure with lower carbon percentages which leads in 4–12 times high value addition to graphite. This technique can be applied to vein graphite rich in silicate minerals (especially along the wall zones of graphite veins) which are considered as waste of mining products. Further purification of final graphite product is possible by removing iron components of final FG product by magnetic separation as well as using very fine graphite powders for the flotation process.

Methods

Materials

Vein graphite samples collected from Bogala mines, Sri Lanka, were selected for this study. Morphologically different samples such as (a) flakes of radial graphite (b) flakes of striated graphite and (c) needle-platy graphite attached to the wall rock were subjected to the study.

Purification of graphite by floatation method

Coarse samples from each variety were broken into small chips and crushed in a ball mill for 20 minutes to form powders. The grinding time was deliberately selected to be short in order to prevent the changes that may result to the structure of graphite due to mechanical shear. Particle size fraction less than 63 μm was used. PG samples were subjected to continuous stirring in de-ionized water. It has been observed that fine particles of graphite are then dispersed in the solution and coarser particles are settled at the bottom of the container. A glass rod was dipped in the suspension and the suspension was shaken by rotating the glass rod about the vertical axis. Then the fine particles were found to move upwards with the air bubbles generated by the glass rod technology. These fine particles were eventually floated on the

surface of water. This flotation technique does not require any chemicals for froth formation nor does it require chemicals for specific gravity adjustments.

Characterization

X-ray diffraction (XRD) patterns were recorded using powder diffraction machine, Rigaku, (RINT-TTR III), under Cu Kα radiation (λ = 1.5406 Å). Raman spectroscopy measurements were taken using a Renishaw InVia Reflex Raman microscopy system with a 532 nm laser. Fourier transform infrared (FT-IR) spectra were collected using an IR Prestige-21 Shimatzu FT-IR spectrophotometer. Field-emission scanning electron microscopy along with energy dispersive X-ray spectroscopy (EDS) were done by FE-SEM, Hitachi S-4700. Transmission electron microscopic (TEM) images were obtained on a JEM-2100 electron microscope (JEOL Ltd. Japan), at an accelerating voltage of 200 kV. The specimen was prepared by dispersing graphite powders in ethanol to form a suspensions followed by ultrasonication for 1 h A drop from each sample was put, separately, on carbon film-coated copper grids for observation. The high-resolution images of periodic structures were analysed and filtered by the Fast Fourier Transformation (FFT) method. X-ray photoelectron spectroscopy (XPS) measurements were performed using PHI 5000 VersaPribe II ESCA with a monochromated Al Kα radiation (hγ = 1486.6 eV) available at Toyota Technological Institute, Japan. Full scans (Binding energies ranging from 0 to 1200 V) were acquired using 1 eV/step, while the higher resolution scans were obtained using 0.025 eV/step. The pressure during acquisition was less than 1 x 10^{-8} Torr. The experimental curves were fitted using Multipack data analysis software. The chemical composition of graphite samples were analyzed by Inductively Coupled Plasma Mass Spectrophotometry (ICP-MS- Perkin Elmer Sciex ELAN- 6000) at Activation Laboratories Ltd., Ontario, Canada. Detection limits for the ICP-MS was ranged between 0.2-0.001 ppm for trace elements.

Declarations

ACKNOWLEDGEMENTS

We thank International Research Centre, University of Peradeniya, Sri Lanka for financial support [InRC/RG/14/01].

Author contributions

G.R.A.K., H.M.G.T.A.P., B.K., M.M.M.G.P.G.M., R.M.G.R., let the research study and prepared the manuscript. H.-H.H., K.K.H.D.S., characterized the samples under supervision of M.Y. All the authors discussed the results and commented on the manuscript.

Competing interests

The authors declare no competing interests.

References

1. Simandl G J, Paradis S, Akam C. Graphite deposit types their origin and economic significance. In: Simandl, GJ, Neetz M, eds. Proceedings of Symposium on Strategic and Critical Materials. USA: British Columbia 163–171 (2015).
2. Sutphin D M, Bliss J D. Disseminated flake graphite and amorphous graphite deposit types. An analysis using grade and tonnage models. CIM Bull. 83, 85–89 (1990).
3. Dissanayake C B. The origin of graphite of Sri Lanka. Org. Geochem. 3, 1–7 (1981).
4. Luque F J, Huizenga J M, Crespo-Feo E, Wada H, Ortega L, Barrenechea J F. Vein graphite deposits: geological settings, origin, and economic significance. Miner. Depos. 49, 261–277 (2014).
5. Dissanayake C B, Gunawardena R P, Dinalankara D M S K. Trace elements in vein graphite of Sri Lanka. Chem. Geol. 68, 121–128 (1988).
6. Lu X, Forssberg E. Preparation of high-purity and low-sulphur graphite from Woxna fine graphite concentrate by alkali roasting. Miner. Eng. 15, 755–757 (2002).
7. Kim B G, Choi S K, Park C L, Chung H S, Jeon, H S. Inclusion of Gangue Mineral and Its Mechanical Separation from Expanded Graphite. Part. Sci. Technol. 21, 341–351 (2003).
8. Wakamatsu T, Numata Y. 1991. Flotation of graphite. Miner. Eng. 4, 975–982 (1991).
9. Florena F F, Syarifuddin F, Hanam E S, Trisko N, Kustiyanto E, Fenda F, Syarifuddin F, Hanam E S, Trisko N. 2016. Floatability study of graphite ore from southeast Sulawesi Indonesia. AIP Conference Proceedings 1712, 050005 https://doi.org/10.1063/1.4941888 (2016).
10. Pugh, R.J. Non-ionic polyethylene oxide frothers in graphite flotation. Miner. Eng. 13, 151–162 (2000).
11. Park J G, Dodd D S. 1994. The merelani graphite project-Tanzania. Miner. Eng. 7, 371–387 (1994).
12. Paulson O, Pugh R J. 1996. Flotation of Inherently Hydrophobic Particles in Aqueous Solutions of Inorganic Electrolytes. Langmuir 12, 4808–4813 (1996).
13. Acharya B C, Rao D S, Prakash S, Reddy P S R, Biswal S K. 1996. Processing of low grade graphite ores of orissa, India. Miner. Eng. 9, 1165–1169 (1996).
14. Vasumathi N, Vijaya Kumar T V, Ratchambigai S, Subba Rao S, Bhaskar Raju G, Flotation studies on low grade graphite ore from eastern India. Int. J. Min. Sci. Technol. 25, 415–420 (2015).
15. Jara A D, Betemariam A, Woldetinsae G, Yong J. Application and current market trend of natural graphite: A review. Int. J. Min. Sci. Technol. 29, 671–689 (2019).

Figures

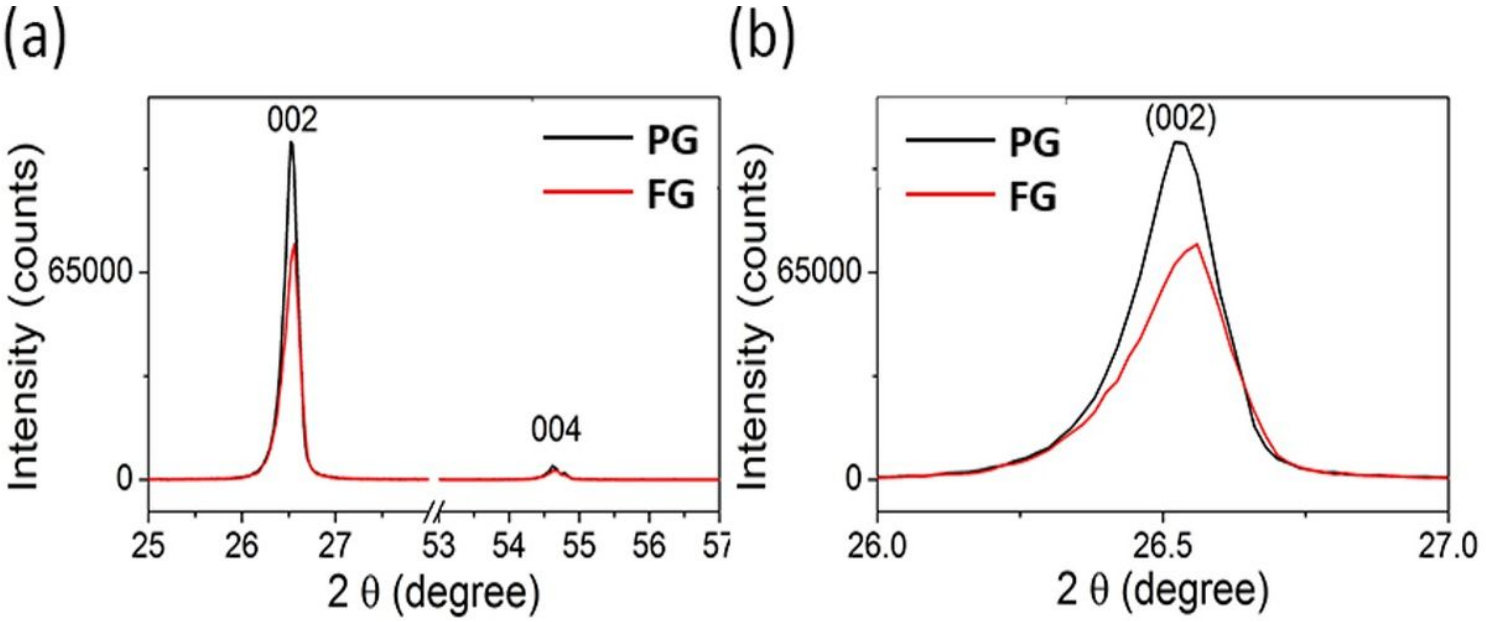

Figure 1

(a) XRD patterns of the PG and FG samples. (b) The enlarged (002) reflections used for the calculation of crystallite size.

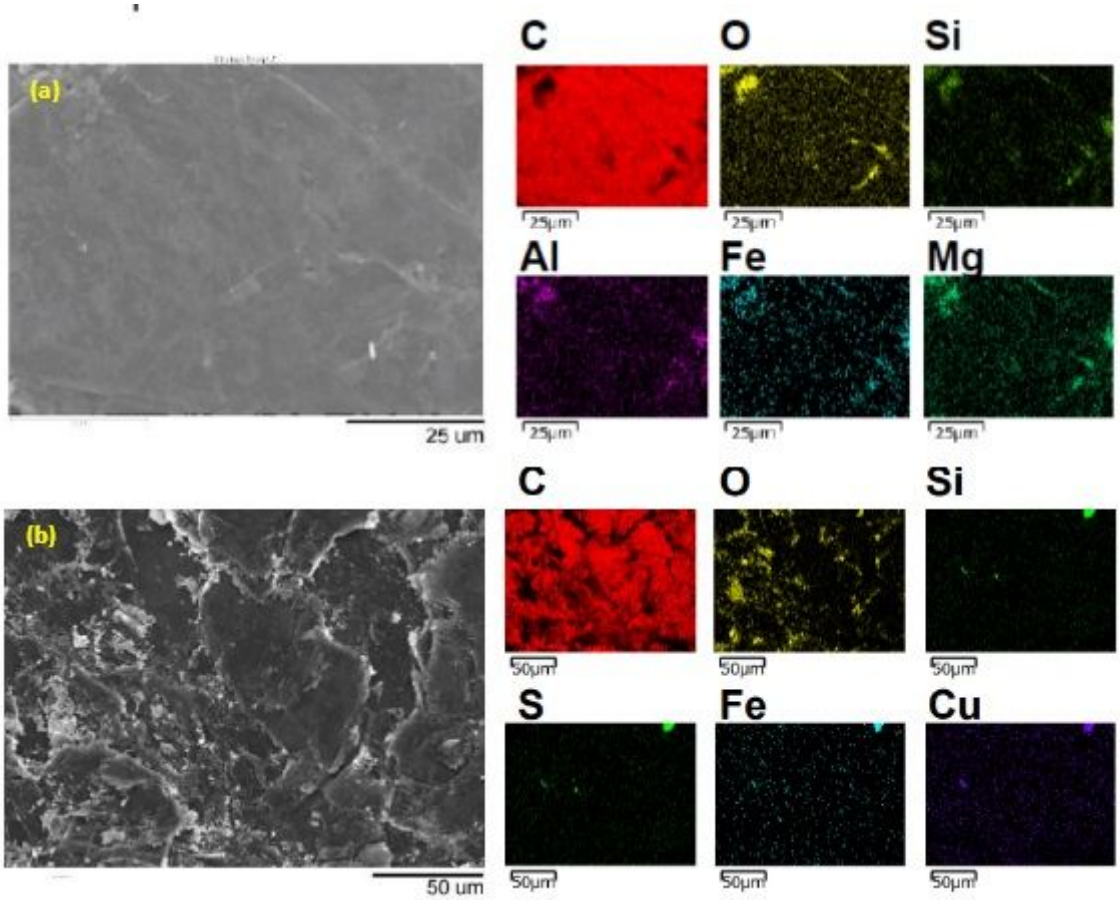

Figure 2

SEM and EDS images of vein graphite samples from two locations before grinding to prepare PG.

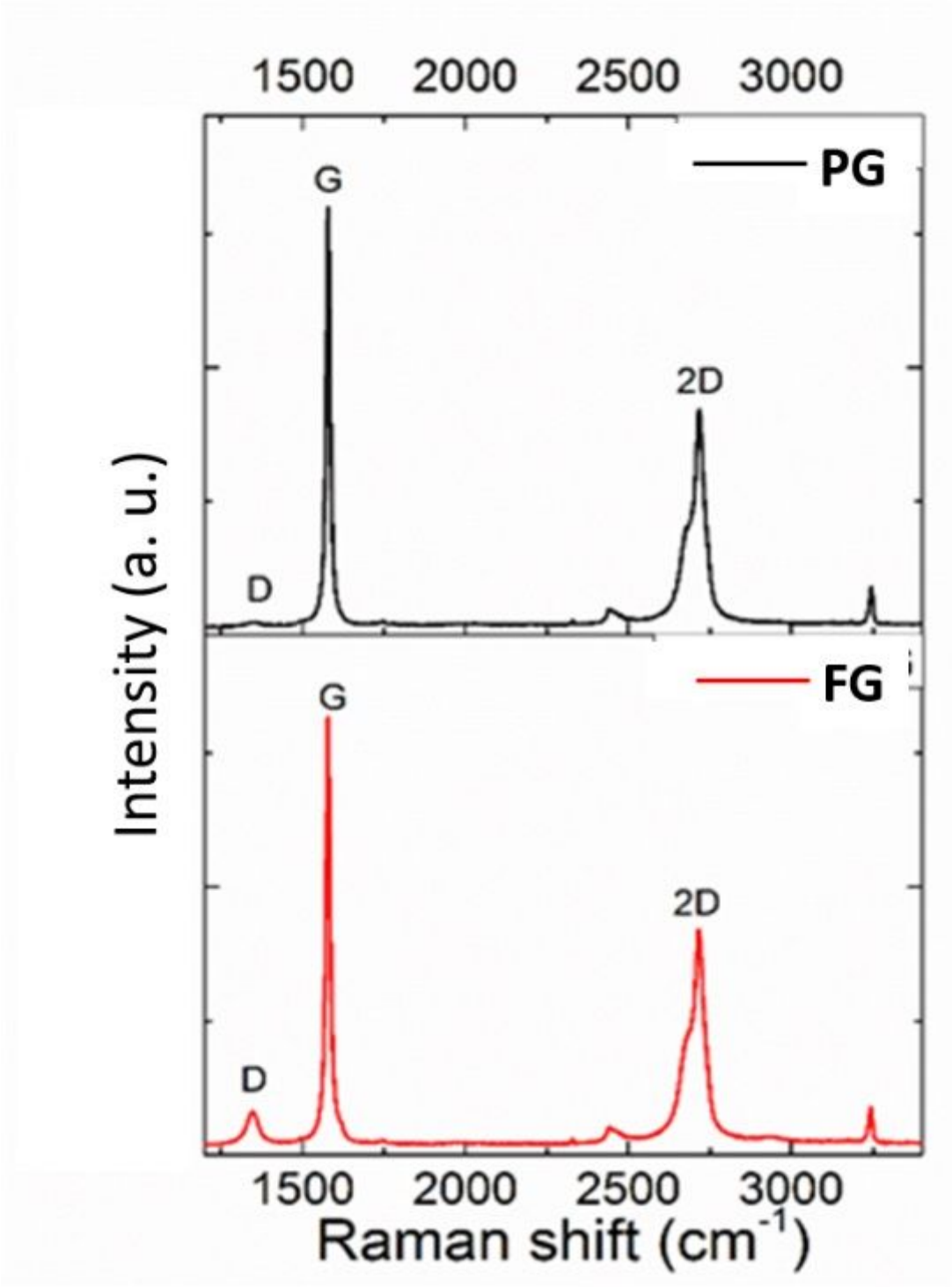

Figure 3

Raman spectra of (a) PG and (b) FG samples. The D peak appears in FG sample due to the edge effects.

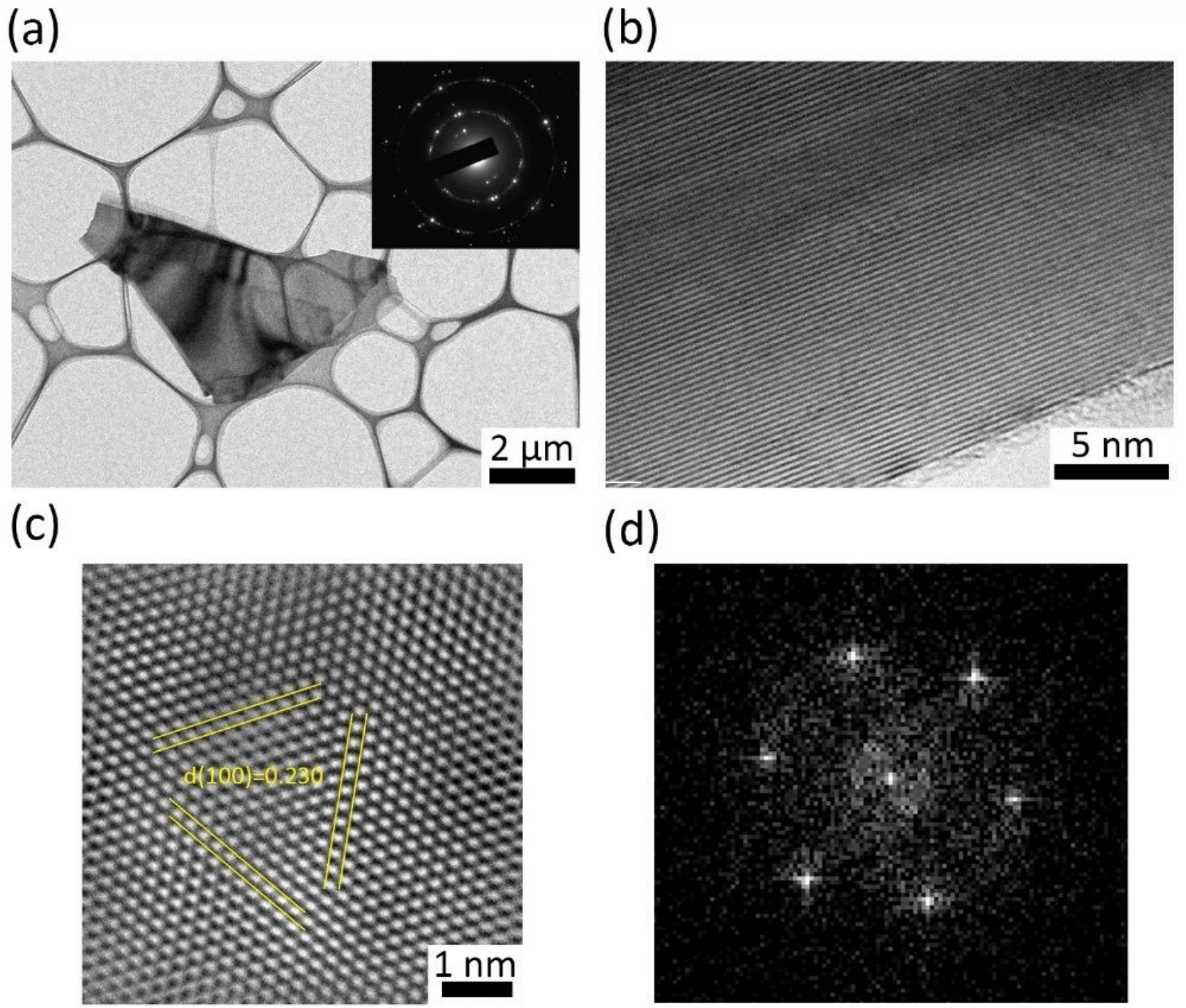

Figure 4

(a) Low-magnification bright-field TEM image of the PG specimen with an inset of corresponding [0001] electron diffraction pattern. (b) TEM image of the folded edges for the PG specimen. (c) Fourier filtered high resolution TEM image and (d) the corresponding FFT image.

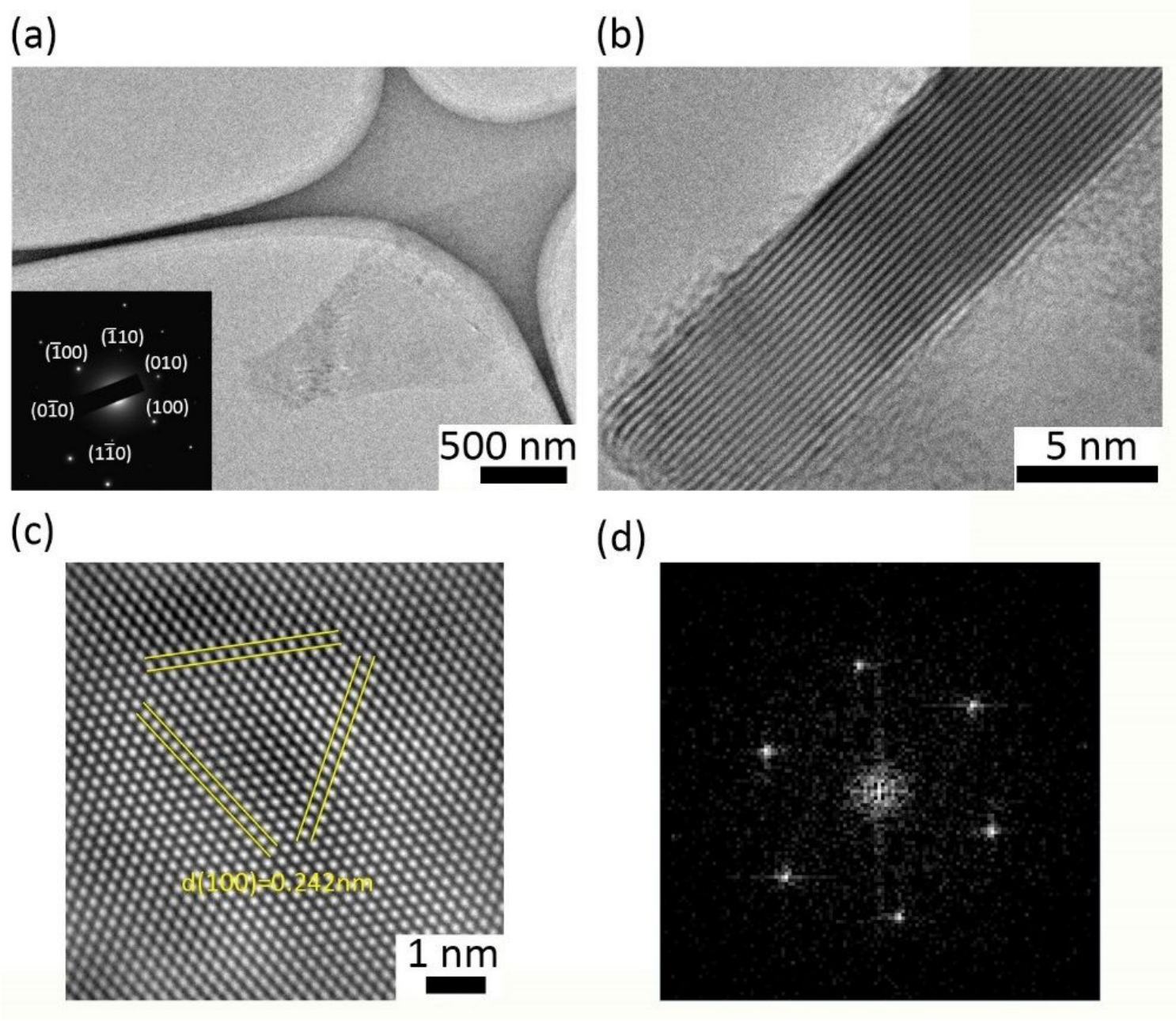

Figure 5

(a) Low-magnification bright-field TEM image of the FG specimen. The inset is the corresponding selected-area electron diffraction pattern showing the primarily single crystalline nature. (b) High resolution TEM image of the edge of the flakes consisting approximately 16 layers. (c) Fourier filtered high resolution TEM image of the FG and (d) the corresponding FFT image.

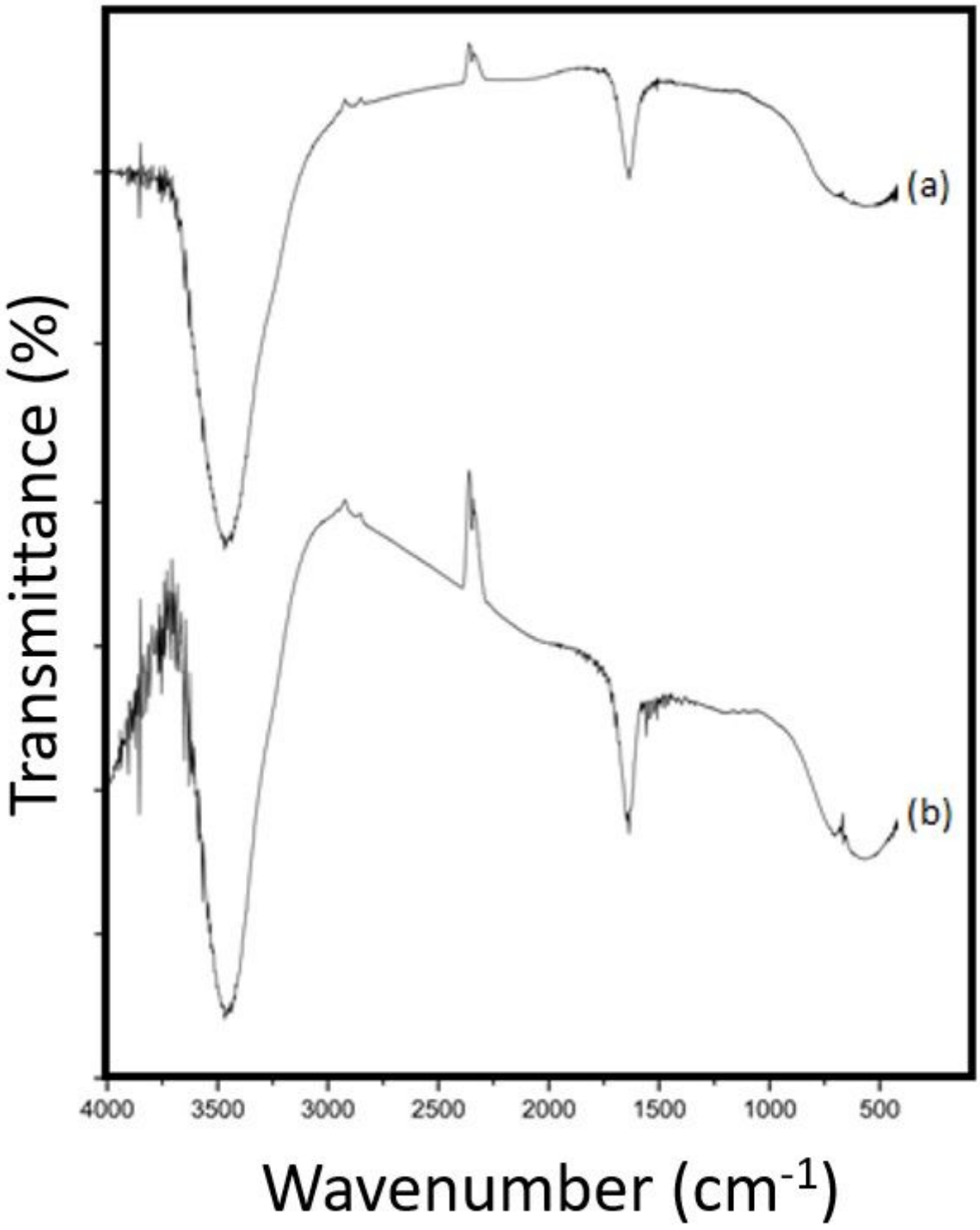

Figure 6

FT-IR spectra of (a) PG and (b) FG

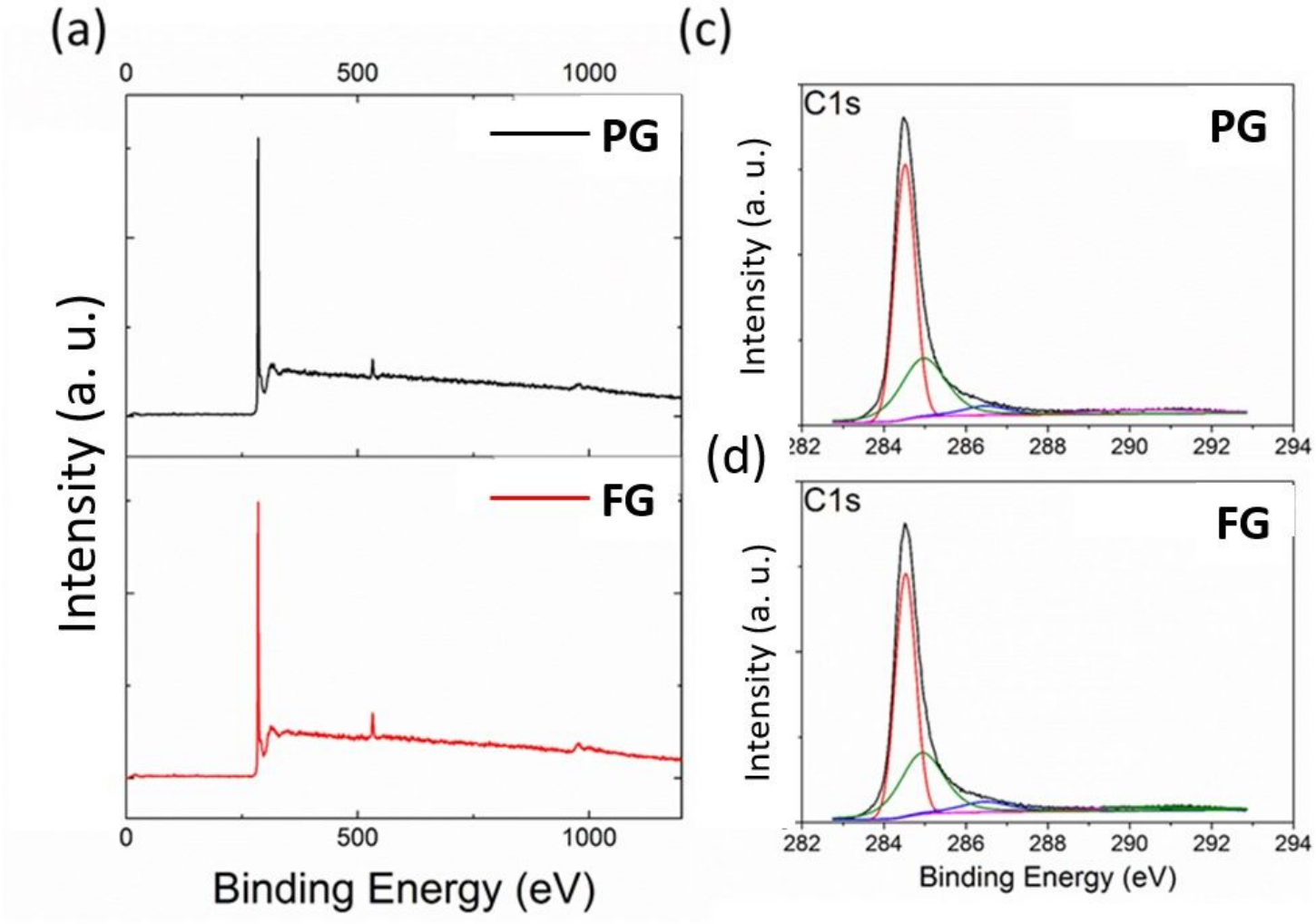

Figure 7

XPS survey spectra of (a) PG and (b) FG samples. Deconvoluted C1s spectra of (c) PG and (d) FG samples.